Bulletin of the Seismological Society of America, Vol. 99, No. 6, pp. 3140–3149, December 2009, doi: 10.1785/0120080262

Test of Seismic Hazard Map from 500 Years of Recorded Intensity Data in Japan

by Masatoshi Miyazawa and Jim Mori

Abstract Maximum seismic intensity maps for Japan are constructed using the recorded intensity data from 1498 to 2007 and are used to test the probabilistic seismic hazard map (PSHM) by the Headquarters for Earthquake Research Promotion, Japan. The historical intensity maps are compared with the hazard maps of probable maximum seismic intensity for a 475-yr return period, assuming a Poisson distribution (10% in 50 yrs). We look at cases that include all events, only subduction zone earthquakes, and all events excluding subduction zone earthquakes. The megathrust earthquakes in the subduction zones produce large bands of high intensities along the Pacific coast side, while onshore crustal earthquakes create a patchy distribution of large intensities over all of Japan. The maximum recorded intensity map for the past 500 yrs and the maximum predicted intensity map for the ~500-yr return period from the PSHM are very similar for the cases including all events and the subduction zone earthquakes, while there is poor correlation for the third category that includes mostly onshore crustal earthquakes. If we consider only the amount of area, not the specific locations, the recorded intensity map and the PSHM (using the maximum case) have a high degree of correlation for Japanese Meteorological Agency (JMA) intensity higher than 4 for all of the cases. Statistically, the present hazard maps for Japan seem to agree with the past intensity distributions and can be regarded as appropriate hazard maps, even though there may be strong dependencies on uncertain model parameters for the PSHMs.

Introduction

Recently, seismic hazard maps based on various models for many regions have been produced to provide useful information on future probable ground motions (e.g., Frankel *et al.*, 1996; Global Seismic Hazard Assessment Program, 1999; Headquarters for Earthquake Research Promotion, 2005). The maps generally include a probabilistic estimation of earthquake occurrence over a certain spatiotemporal range and strong ground motion estimates using attenuation relations. Producing a hazard map is a challenge because there are many uncertain variables for specifying the forthcoming earthquakes. Although geological, geophysical, and paleoseismic studies are capable of identifying the locations of faults that can cause large earthquakes, and estimating source parameters, it is difficult to provide a deterministic model that specifies future earthquakes. Also the accurate estimation of ground motions using attenuation relations and site effects information has significant uncertainties. Still, information about future earthquake shaking is crucially needed for populated areas where the risk of the earthquake damage is relatively high, so it has been necessary to produce hazard maps based on various models that contain many parameters of varying reliability.

In Japan, the Headquarters for Earthquake Research Promotion (HERP) published in 2005 probabilistic seismic hazard maps (PSHMs), as well as shaking distributions from scenario earthquakes. The PSHMs are revised annually, updating the recent seismicity and including new geological information about active faults. The maps show the expected ground motions from future subduction zone earthquakes and onshore crustal earthquakes, considering the estimated recurrence intervals of those events (Fujiwara *et al.*, 2006). However, in Japan, there have been no tests of the seismic hazard maps to validate the models. For example, in California the Collaboratory for the Study of Earthquake Prediction (CSEP) Testing Center is developing methodologies to evaluate such types of forecasts (Field, 2007; Jordan *et al.*, 2008).

Because earthquakes repeatedly occur on active faults, the most model-independent estimate of the future maximum intensity distribution is to use a record of past events over a long period (Kawasumi, 1951). We can reliably characterize the probable future event locations, magnitudes, and source mechanisms for the events if there is a long record of data, where long is defined as spanning multiple earthquake cycles for a given source. Seismic hazard maps based on a model

without empirical justification may be inappropriate (Freedman and Stark, 2003); however, historical data can overcome this difficulty. Also the recorded intensity includes site effects that play an important role in estimating the ground motion. Hence, a map of the distribution of maximum intensities, based on data recorded for a period longer than or comparable to the earthquake recurrence interval, is capable of showing the probabilistic ground shaking in the future and can be also used for testing probabilistic hazard maps.

Miyazawa and Mori (2006) combined the recorded historical intensities in Japan from the catalog of Usami (2003), which compiles written historical records, with the Japan Meteorological Agency (JMA) intensity catalog. These data were used to make a maximum recorded intensity map covering the period from 1586 to 2004. The map can be viewed as a simple hazard map that has essentially no model dependence, as mentioned previously. This map used a spatial grid model with about 5–7 km intervals because of the relatively sparse data points, especially for the historical data, so that it may not be adequate to directly compare this map to the fine spatial resolution of the hazard maps by HERP. The time period of about 400 yrs does not adequately cover the recurrence intervals of onshore faults, which are typically thousands of years; however, it is still one of the best data sets to study the long-term occurrence of earthquakes in Japan.

The purpose of this article is to compare the records of historical maximum intensities for the past 500 yrs with the predicted maximum intensities from the HERP hazard map. In this study we modify the recorded intensity map of Miyazawa and Mori (2006) by taking into account the site effects at the interpolated locations where the intensities are not directly recorded. Because the site effects are empirically included at the recorded locations, we only need to provide relative values for the site effects for the interpolated points. With this procedure we can obtain a better distribution of seismic intensity with high spatial resolution, even at locations where intensities were not recorded for past earthquakes. We also add some additional data from historical and recent earthquakes to extend the time period from 1498 to 2007. These revised historical maximum intensity maps are then compared to the HERP hazard maps of 1 January 2008. The time period of the historical data is not adequate to see recurrent earthquakes on the same fault; however, the large spatial area helps to compensate for the short period. For this reason, in addition to comparisons for specific locations, we also show comparisons of the areal averages of the intensity levels.

There are a number of examples of seismic hazard maps using historical intensity data in Italy, New Zealand, the United States, and Japan (e.g., Monachesi *et al.*, 1994; Papoulia and Slejko, 1997; Stirling and Petersen, 2006; Bozkurt *et al.*, 2007), based on grid and site-based intensity exceedance rate methods, where the large intensities and their frequency are estimated from extrapolating the lower values of intensity. Our purpose here is not to make such a seismic hazard map but to simply test the present Japanese hazard map, which has been produced by a very different approach, by comparison to the historical intensity data.

In this article we use two kinds of JMA seismic intensities: scale intensity (I) and instrumental intensity (I_0). The original JMA intensity (I) had eight divisions from 0 to 7 and was in use until 1996, undergoing minor changes. This intensity qualitatively reflects the amount of damage caused by the earthquakes. Since 1996, there are now 10 divisions of the intensity scale, with intensity 5 and 6 split into 2 levels each and designated by $I = 5$ lower (5−), 5 upper (5+), 6 lower (6−), and 6 upper (6+). I_0 is an instrumental value derived from seismograms of the ground motion. The instrumental intensity was designed to correspond directly to I and has been used since 1996. For older earthquakes before 1925 when the JMA intensity records are not available, intensity I can be assigned by evaluating historical written records of the damage, as was done by Usami (2003). Also we can estimate I_0 on average from I. Moreover, the JMA intensity can approximately be related to the modified Mercalli (MM) intensity and peak acceleration.

Data and Method

We use intensity data in Miyazawa and Mori (2006) from 1586 to 2004, with additions of the intensity distributions recorded back to 1498 (Usami and Daiwa Exploration and Consulting Co. Ltd., 1994; Usami, 2003) and recent earthquakes from 2005 to 2007. A total of 551 earthquakes are selected (Figs. 1 and 2), where the maximum intensity of each event is equal to or larger than 5−. Miyazawa and Mori (2006) use the JMA intensity values for events from 1926 and Usami's catalog (2003) for earlier historical earthquakes. For intensity values from 1926 to 1996, we assume intensity 5 and 6 to be intensity 5− and 6−, respectively, because we are interested in values that do not exceed actual maxima. This assumption may cause some of the intensity data to be underestimated. We will discuss effects of this lower estimation in the Discussion section. For older historical events, Usami (2003) uses intermediate values that we assume to correspond to the present split levels. For recent events, instrumental intensities measured by K-NET are also combined in our data set. K-NET is a high density accelerometer network deployed by the National Research Institute for Earth Science and Disaster Prevention (NIED) to record the strong ground motions at about 1000 stations over all of Japan.

The present instrumental JMA seismic intensity (I_0) is calculated from envelope waveforms of data with a velocity-acceleration filter (band-pass filter around ~1 Hz) by

$$I_0 = 2 \log A + 0.94, \tag{1}$$

where A is the amplitude exceeded for a cumulative duration time of 0.3 sec. We assume a linear relationship between the amplitude and the time lag for the envelope waveform. If the amplification factor c is given at a site, the instrumental intensity is increased by $2 \log c$ compared to the reference

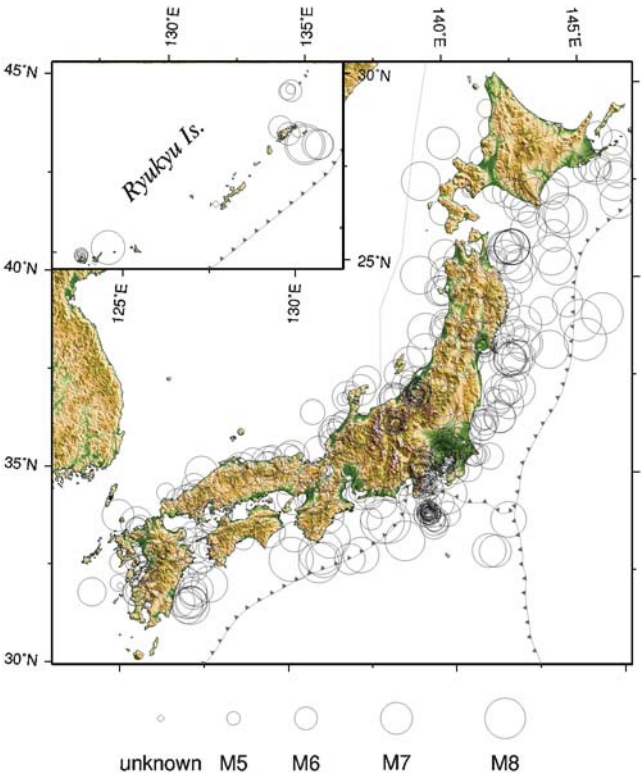

Figure 1. Epicenters of earthquakes from 1498 to 2007 used in this study (551 events). The inset map shows Ryukyu Islands to the southwest of the main Japan Islands.

instrumental intensity at an equivalent hard rock site, and conversely the reference instrumental intensity can be obtained from I_0 on the surface by subtracting $2 \log c$.

The modified instrumental intensity maps are estimated on a fine mesh in the following process (Fig. 3). We first calculate the reference instrumental intensities at each station for each event. The reference instrumental intensity for every grid area of size $2^{-6} \times 2^{-6}$ deg^2 (about 1.7×1.4 km^2) is

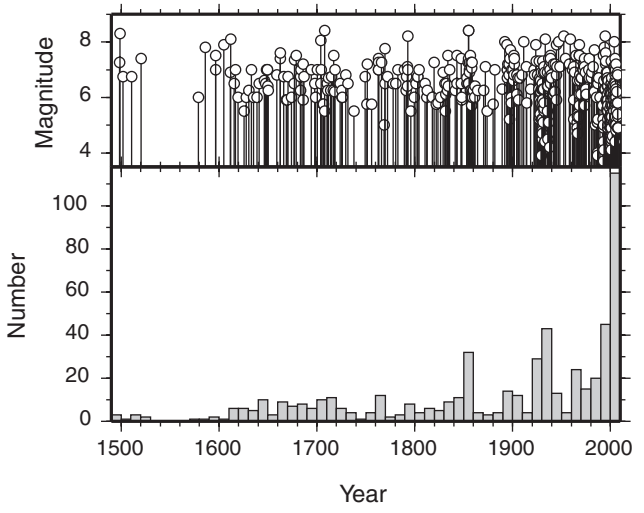

Figure 2. Magnitude and number of earthquakes. Magnitudes of historical earthquakes likely have large uncertainties.

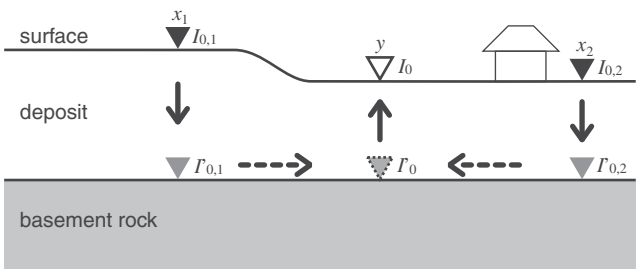

Figure 3. Schematic illustration of the process to obtain the instrumental intensity I_0 at point y from the recorded instrumental intensity $I_{0,i}$ at x_i. Prime ($\prime$) denotes the reference intensity at the basement rock after removing the site effect.

calculated by a method using linear interpolations of the surrounding recorded data based on Miyazawa and Mori (2006). The grid interval is 4 times as fine as that used in the previous study. We also modified equation (1) by Miyazawa and Mori (2006) to obtain the reference instrumental intensity I'_0 at a location y from intensities at n surrounding locations as

$$I'_0 = \frac{\sum_{i=1}^{n}\left[(\sum_{j=1}^{n} \|x_i - x_j\| / \|y - x_i\|) I'_{0,i}\right]}{\sum_{i=1}^{n}(\sum_{j=1}^{n} \|x_i - x_j\| / \|y - x_i\|)}. \quad (2)$$

$I'_{0,i}$ is the reference instrumental intensity at x_i, where intensity $I_{0,i}$ at the ith location is recorded, after removing the site effect. Equation (2) can both evaluate distances of other observations from y and avoid biases due to the clustering observation points. For each earthquake, a reference instrumental intensity map is thus obtained, then the site effect is included with the amplification coefficient for each grid area to produce the intensity map for the earthquake. For the amplification coefficients, we use the site data by Kubo *et al.* (2003), which are also used to make the HERP probabilistic maps. To account for potential uncertainties of recording location and site amplification, we use an amplification coefficient that is an average value including the surrounding adjacent grid points. The interpolated intensity would have an error of about ± 1 in intensity level. These interpolated intensities are not real data, but we use the term "recorded" data for both these interpolated values and the actual recorded data.

Maximum Recorded Intensity Maps with Site Effects

The modified maximum intensity maps from the earthquakes that occurred from 1498 to 2007 are shown in Figure 4, including a map of all events (Fig. 4a), a map of only events identified as subduction zone earthquakes (Fig. 4b), and a map of all events excluding the subduction zone events (Fig. 4c). The third category includes the onshore crustal earthquakes, volcanic events, and unknown events. In Figure 4a,b, high intensity regions with $I \geq 5+$ extend along the Pacific coast side of Japan due to the repeating large megathrust earthquakes along the plate boundaries. Areas in white indicate

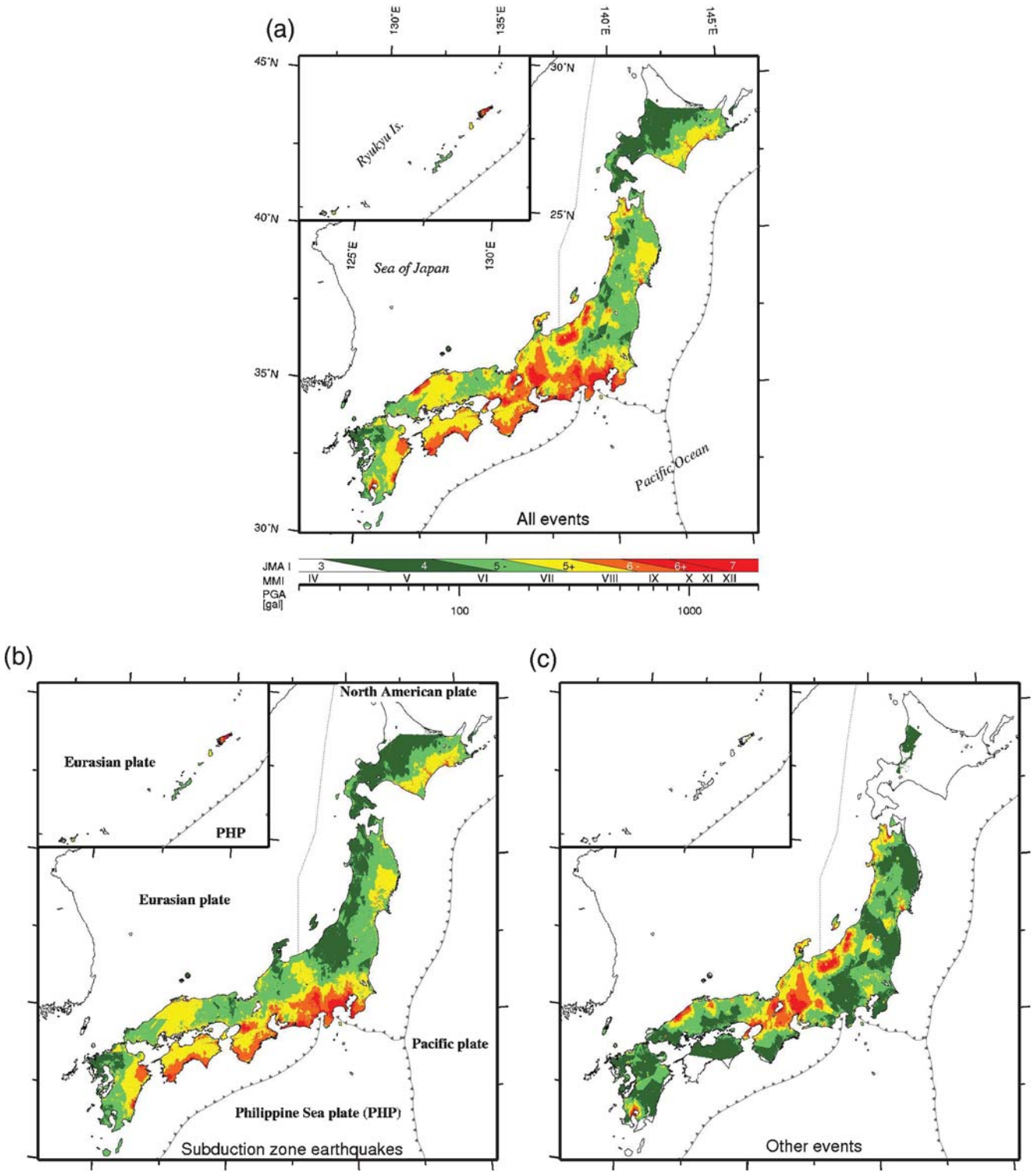

Figure 4. Maps of maximum recorded intensities for 1498–2007: (a) all earthquakes; (b) earthquakes in interplate regions and within the subducting slabs; and (c) other events (e.g., earthquakes on onshore active faults, volcanic events, back-arc basin earthquakes). The color scale indicating JMA intensity and associated MM intensity and peak ground acceleration are shown on below (a). Areas in white indicate where there are almost no values or JMA intensity < 4.

where there are almost no values or $I < 4$. Actual numbers of events used to make the maps are 256 out of a total of 551 for the all events category, 105 out of 200 for subduction zone earthquakes, and 222 out of 351 for the other events category.

Even if we do not have a high density of actual recorded intensity values, the resultant maps can clearly show the plausible patterns of the distribution. For example, one can generally find higher intensities in basins with thick

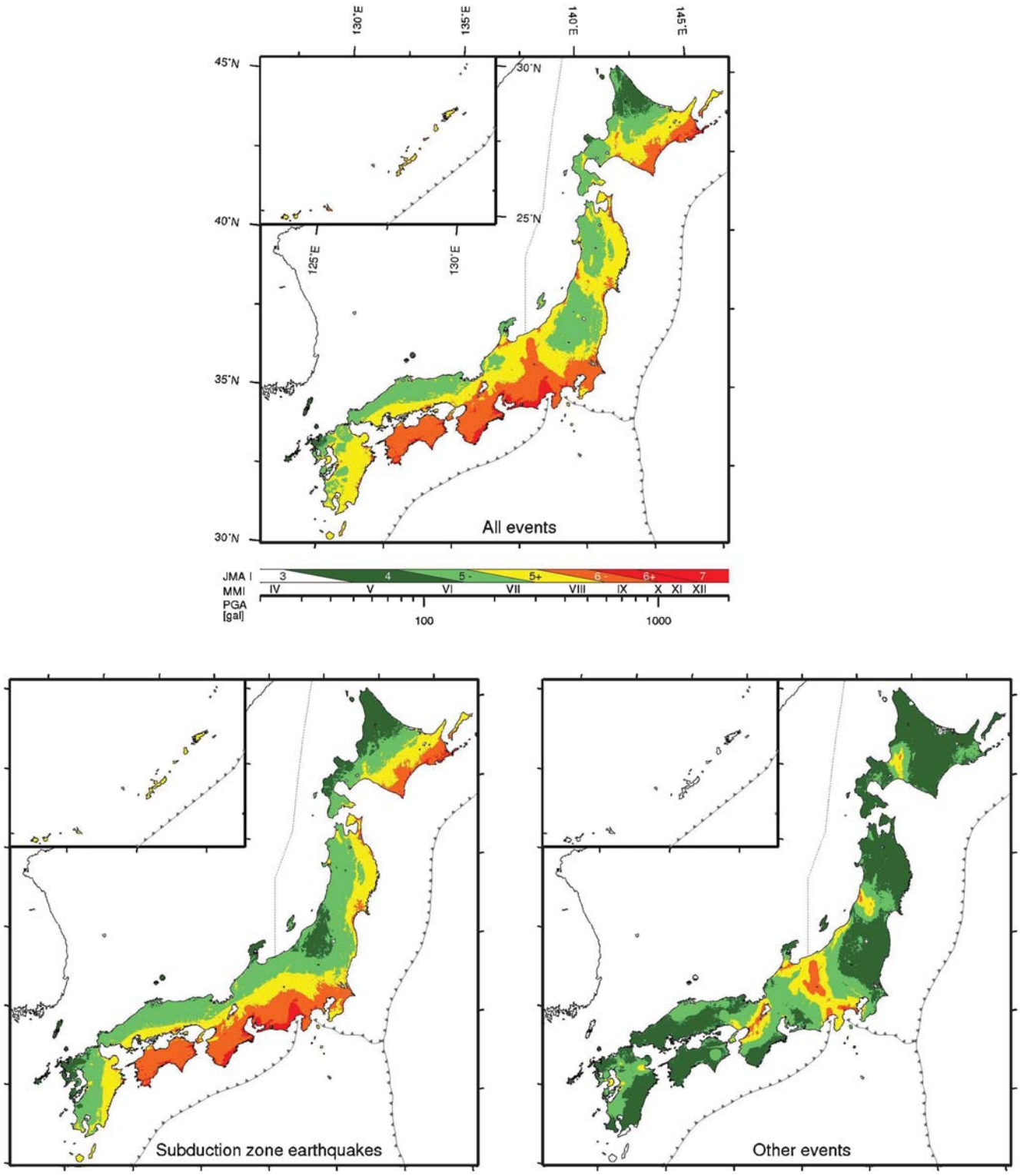

Figure 5. Seismic intensity maps for a 10% probability of exceedance in 50 yrs as of 1 January 2008. Maps are illustrated using data from the Japan Seismic Hazard Information Station (see the Data and Resources section).

sedimentary deposits and lower intensities in the mountain areas (see the topography in Fig. 1), which is an improvement of the maps in Miyazawa and Mori (2006). More than 90% of the region is calculated by the interpolation process. Because of the simple method for linear interpolation, which needs a good azimuthal spread of surrounding recorded values, areas close to the coast may not be included for calculating the intensity for some events and the values there may be underestimated in the maximum intensity maps.

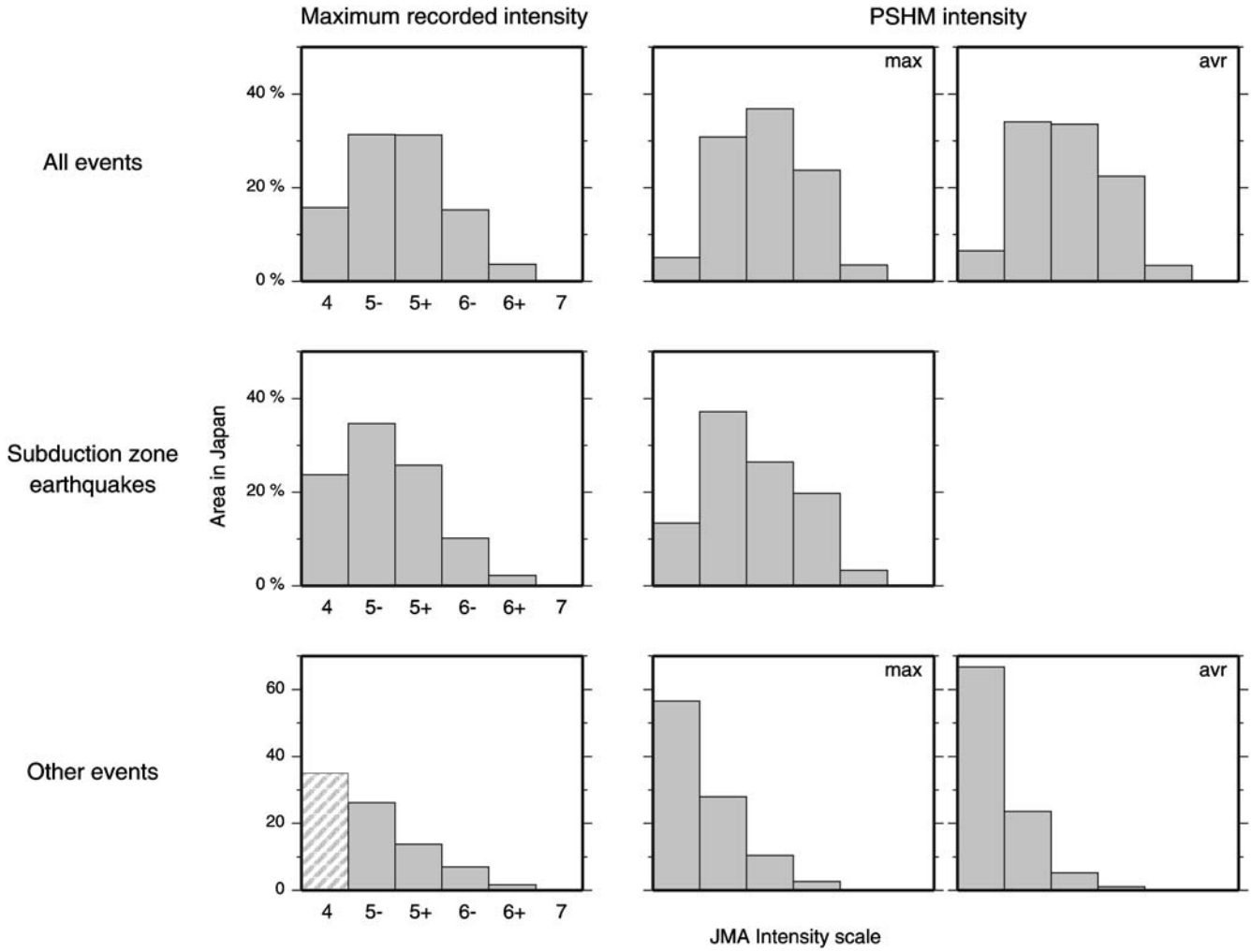

Figure 6. Cumulative area distributions of different levels of intensity for all events (top row), subduction zone earthquakes (middle row), and other events (bottom row). The data for the left-hand column of histograms were obtained from Figure 1. Max and avr indicate values from the maximum and average versions of the PSHM, respectively.

Examples of the HERP probabilistic maps as of 1 January 2008 are given in Figure 5, which shows seismic intensities for a 10% probability of exceedance in 50 yrs. The intensity values are equivalent to the maximum seismic intensity for a 475-yr return period if we assume a Poisson distribution. We examine the PSHMs by directly comparing maps in Figures 4 and 5. In terms of testing the PSHMs, we think that this approach is the most straightforward method because there is a relatively large amount of observed intensity data, rather than trying to make maps that infer the maximum intensity by extrapolation from the distribution of the lower intensity data (e.g., Monachesi *et al.*, 1994).

To statistically compare the recorded intensity map with the PSHM, we first look at the frequency of exceedance of the maximum intensity. Figure 6 shows the histograms of the intensity values from the maximum intensity maps in Figure 4 and those from the PSHM for the 475-yr return period. The histograms for all events and subduction zone earthquakes are quite similar. For example, in the category of all events, $I \geq 5-$ is 82% of the area for the recorded intensity, 95% of the area for the maximum PSHM, and 93% of the area for the average PSHM. For $I \geq 6-$, the values are 20%, 27%, and 26%, for the recorded intensity, maximum PSHM, and average PSHM, respectively. Maximum and average cases of the PSHMs denote maximum and average estimates of earthquake source parameters for onshore crustal earthquakes with large uncertainties in the recurrence intervals and magnitudes. For subduction zone earthquakes, $I \geq 5-$ have values of 73% and 87% for the recorded intensity map and PSHM, respectively. $I \geq 6-$ have values of 13% and 23% for the recorded intensity map and PSHM, respectively. For the category of other events, which includes mostly onshore crustal earthquakes, the area of higher intensity becomes much less. The recorded intensity and the PSHM have a moderate correlation; for $I \geq 5-$ the values are 49%, 41%, and 30% for the recorded intensity, maximum PSHM, and average PSHM, respectively. For $I \geq 6-$, the values are 9%, 3%, and 1% for the recorded intensity, maximum PSHM, and average PSHM, respectively. For the recorded intensity maps, due to the incompleteness of records, such as the large regions

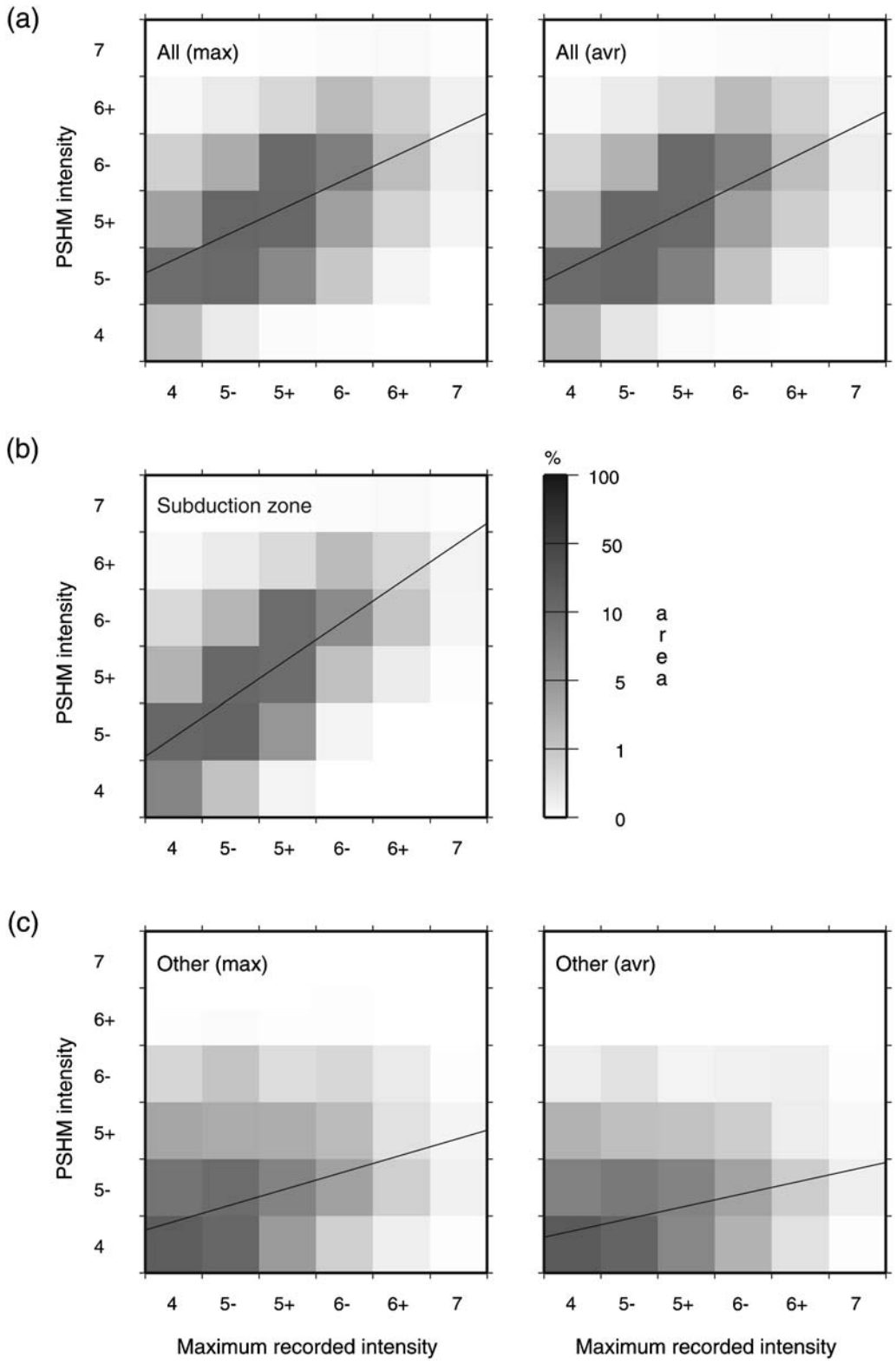

Figure 7. Relationship between the recorded intensity and PSHM intensity at each grid area over Japan, where the intensity is given in both maps. The gray shading shows the percentage of values for each combination of observed intensity and predicted intensity from the PSHMs. The values are normalized by the total area of the recorded intensity in each figure. The line shows the regression fit. High values along the diagonal, symmetry with respect to the diagonal, and a line close to the diagonal indicate high correlation between the two maps for specific locations.

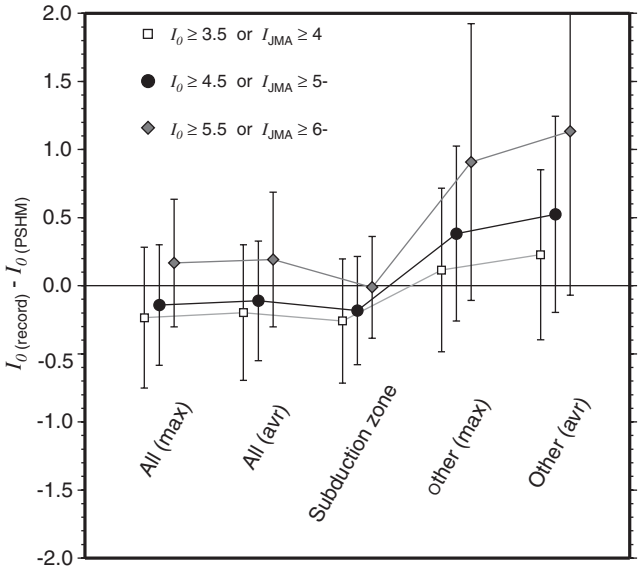

Figure 8. Differences between the maximum recorded intensity and PSHM intensity values for different event categories and different intensity ranges.

with no values in white in Figure 4c, the areas corresponding to JMA intensity 4 and lower cannot be evaluated.

We next compare the maximum recorded intensity maps to the PSHMs for the specific locations where values are given in both maps. Figure 7 shows the relationship between the recorded intensity and the PSHM intensity for all grid areas across Japan. The gray shading shows the number of values for each combination of observed intensity and predicted intensity from the PSHM. The values are normalized by the total area of the recorded intensity in each figure. High correlations are shown when the values of the maximum recorded intensity map equal the values of the PSHM, as shown by the diagonal elements. Because the diagonals are fairly clear and other elements tend to be symmetric with respect to the diagonals in the top three panels, this means there is a fairly high degree of correlation between the observed intensity and PSHM for the specific locations. The actual differences are quantified and shown in Figure 8. Over all events, there are some systematic differences where the recorded intensities are higher than the PSHM values for high intensities and the recorded intensities are lower than the PSHM values for lower intensities (Figs. 7a and 8). There is high correlation for the subduction zone earthquakes (Figs. 7b and 8). The values become especially similar for intensities equal to and larger than 5−. The similarity of the specific location values can also be seen in Figure 6. For the category of other events, we can find high correlation for intensity 4 because this intensity level can be observed anywhere over Japan, while there is no clear correlation for larger intensities (Figs. 7c and 8). However, as was mentioned previously, the recorded historical values for intensity equal to or smaller than 4 are very likely incomplete.

Discussion

Generally there is a high degree of correlation seen between the maximum recorded intensity maps and the PSHMs, and there is especially high correspondence for the subduction zone earthquakes. This is because the historical data recorded for the past 500 yrs is sufficiently longer than the recurrence interval of subduction zone earthquakes, and the modeling used by HERP produces reliable hazard maps for those events. If the recorded intensity is considered to represent the levels of future intensity distribution better than the PSHM, there may be a slight underestimation in the larger intensities and a slight overestimation of the smaller intensities in the PSHM. Although we cannot discount that the variations are due to uncertainties, these trends are reliable especially for the large intensities because we assume older intensity 5 and 6 values to be intensity 5− and 6−, respectively, which would underestimate values for some historical data.

When we look at the category of other events, we find a poor correlation between the recorded intensity map and the PSHM. This is probably mainly because there are not enough historical data to span the recurrence of onshore crustal earthquakes. Also there are difficulties in predicting cycles, accurate locations, and mechanisms of these earthquakes in the PSHM. Looking carefully at Figures 6–8, the PSHM for the maximum case has a higher correlation with the maximum recorded intensity map than the PSHM for the average case. Even though 500 yrs are not enough to fully evaluate the recurrence interval of each crustal fault (~1000–10, 000 yrs), using the historical data over all of Japan provides enough spatial coverage over many faults. Hence, the actual activity of faulting on average could be evaluated even from our data set. It appears that the maximum case for the major faults in the PSHM fits the historical data better. This suggests that these fault parameters are better than those of the average case, and/or there is a more than expected number of unrecognized active faults that are not considered in the present PSHM.

We use the intensity data recorded from 1498 to 2007; however, the numbers of events are not uniform throughout this period, and there are less events for the first few hundred years because of the poorer documentation of the intensity distribution (Fig. 2). This might suggest that the current intensity data is not adequate to infer the maximum intensities over the past 500 yrs; however, the maximum recorded intensities in most of Japan are associated with the large megathrust earthquakes (M_w ~7–8.6) with recurrence intervals of ~50–400 yrs along the Pacific subduction zones, for which there is likely a fairly complete record. As mentioned previously, there may be a deficiency of data for the onshore crustal faults that have recurrence times of thousands of years, but this may be somewhat compensated by the spatial coverage over many faults to obtain reasonable average rates for the whole country.

JMA seismic intensity is determined as mentioned in the section titled Data and Method, so that the intensity values from instrumental observations should agree well with the

historical intensity estimated from damage. However, this intensity value is strongly affected by the ground motions with periods ~1 sec, so the estimation of damage from older earthquakes might not be completely consistent with the damage to more modern structures that include multistory buildings with natural periods longer than 1 sec. The problem might be particularly affected by the long-period waves from large subduction zone earthquakes. However, the good correlation between the two maps for subduction zone earthquakes probably supports the conclusion that the ground motion estimates used in the PSHMs are appropriate.

The present PSHM is a time-dependent hazard map. Even though the historical maximum intensity map supports the results of the PSHMs, these probabilistic maps need to be modified as large earthquakes occur. In this process, there needs to be a subjective judgment whether or not a recent large earthquake is the expected recurrence for a specific fault. In this decision, the characteristic earthquake model may not always be easily applied, as indicated in the debate over the 2005 Miyagi-oki earthquake (e.g., Kanamori *et al.*, 2006; Umino *et al.*, 2006). This also implies that to assess the seismic hazard, a simple estimation of the frequency of high intensities by extrapolating lower intensity data may not always be valid in a specific region.

Conclusions

The maximum recorded intensity maps for the past 500 yrs in Japan, including site effects, are compared with the PSHMs that show the maximum intensity for a 475-yr return period. These two types of maps have a high degree of correlation for the cases that include all events and only the subduction zone earthquakes because intensities recorded for ~500 yrs sufficiently capture the repeated megathrust earthquakes produced by the subduction zone with recurrence intervals of ~50–400 yrs. Also, the recurrence models used for the subduction events in construction of the PSHM are reasonably constrained. There is a poor correlation for the category of other events that mostly include the onshore crustal earthquakes. This may be expected because of the relatively short historical record and the uncertainties in specifying recurrence models in the PSHM. There is a small systematic difference between the historical intensities and the PSHM. For lower intensities levels ($I = 4$) the recorded intensities are lower than the PSHM and for the higher levels ($I \geq 6-$) the recorded intensities are higher than the PSHM. The HERP probabilistic maps have maximum and average value versions, which reflect differences in the estimated expected earthquakes for onshore crustal faults. The historical intensity maps appear more consistent with the maximum value maps if we consider the average areal values and not the specific locations. Generally, the present PSHMs agree well with the maximum recorded intensity maps, especially for the subduction zone earthquakes and when considering the cumulative areas of various intensity levels in Japan for all events.

Data and Resources

The PSHMs by HERP and the site amplification data by Kubo *et al.* (2003) are available from the Japan Seismic Hazard Information Station at www.j-shis.bosai.go.jp (last accessed January 2009). Historical seismic intensity data are digitalized from Usami and Daiwa Exploration and Consulting Co. Ltd. (1994), Usami (2003), and the JMA intensity catalog. The instrumental intensities measured by K-NET are available at www.k-net.bosai.go.jp (last accessed December 2008). Plots were made using the Generic Mapping Tools (www.soest.hawaii.edu/gmt, last accessed February 2007; Wessel and Smith, 1998) and the digital topographic data from the Shuttle Radar Topography Mission (SRTM30 version2) (www2.jpl.nasa.gov/srtm, last accessed February 2009).

Acknowledgments

The comments from two anonymous reviewers and associate editor Ivan G. Wong improved the document. Discussions with K. Shimazaki and C. Smyth helped develop this study. This study is supported by the Kansai Research Foundation for technology promotion.

References

Bozkurt, S. B., R. S. Stein, and S. Toda (2007). Forecasting probabilistic seismic shaking for greater Tokyo from 400 years of intensity observations, *Earthq. Spectra* **23,** 525–546.

Field, E. E. (2007). Overview of the working group for the development of regional earthquake likelihood models (RELM), *Seism. Res. Lett.* **78,** 7–16.

Frankel, A., C. Mueller, T. Barnhard, D. Perkins, E. V. Leyendecker, N. Dickman, S. Hanson, and M. Hopper (1996). National seismic hazard maps, June 1996, *U.S. Geol. Surv. Open-File Rept. 96-532*, 100 pp.

Freedman, D. A., and P. B. Stark (2003). What is the chance of an Earthquake?, in *Earthquake Science and Seismic Risk Reduction*, F. Mulargia and R. J. Geller (Editors), NATO Science Series IV: Earth and Environmental Sciences, Vol. **32**, Kluwer, Dordrecht, The Netherlands, 201–213.

Fujiwara, H., S. Kawai, S. Aoi, N. Morikawa, S. Senna, K. Kobayashi, T. Ishii, T. Okumura, and Y. Hayakawa (2006). National seismic hazard maps of Japan, *Bull. Earthq. Res. Inst. Univ. Tokyo* **81,** 221–232.

Global Seismic Hazard Assessment Program (1999). http://www.seismo.ethz.ch/GSHAP/ (last accessed September 2008).

Headquarters for Earthquake Research Promotion (2005). *National Seismic Hazard Maps for Japan*, http://www.jishin.go.jp/main/chousa/06mar_yosoku-e/index-e.htm (last accessed September 2008).

Jordan, T. H., M. Gerstenberger, M. Liukis, P. Maechling, D. Schorlemmer, S. Wiemer, J. Zechar, and The CSEP Collaboration (2008). Collaboratory for the study of earthquake predictability (CSEP), in *Proc. of the 2008 Risk Management Solutions Science Symposium "Advances in Earthquake Forecasting"*, New York, 23 January 2008, 31–33.

Kanamori, H., M. Miyazawa, and J. Mori (2006). Investigation of the earthquake sequence off Miyagi prefecture with historical seismograms, *Earth Planets Space* **58,** 1533–1541.

Kawasumi, H. (1951). Measures of earthquake danger and expectancy of maximum intensity throughout Japan as inferred from the seismic activity in historical times, *Bull. Earthq. Res. Inst. Univ. Tokyo* **29,** 469–482.

Kubo, T., Y. Hisada, A. Shibayama, M. Ooi, M. Ishida, H. Fujiwara, and K. Nakayama (2003). Development of digital maps of site amplification factors in Japan, and their applications to early strong motion estimations, *Zisin* **56,** 21–37 (in Japanese with English abstract).

Miyazawa, M., and J. Mori (2006). Recorded maximum intensity maps in Japan from 1586 to 2004, *Seism. Res. Lett.* **77,** 154–158.

Monachesi, G., L. Peruzza, D. Slejko, and M. Stucchi (1994). Seismic hazard assessment using intensity point data, *Soil Dyn. Earthq. Eng.* **13,** 219–226.

Papoulia, J., and D. Slejko (1997). Seismic hazard assessment in the Ionian Islands based on observed microseismic intensities, *Nat. Hazards* **14,** 179–187.

Stirling, M., and M. Petersen (2006). Comparison of the historical record of earthquake hazard with seismic hazard models for New Zealand and continental Unites States, *Bull. Seismol. Soc. Am.* **96,** 1978–1994.

Umino, N., T. Kono, T. Okada, J. Nakajima, T. Matsuzawa, N. Uchida, A. Hasegawa, Y. Tamura, and G. Aoki (2006). Revisiting the three $M \sim 7$ Miyagi-oki earthquakes in the 1930s: Possible seismogenic slip on asperities that were re-ruptured during the 1978 $M = 7.4$ Miyagi-oki earthquake, *Earth Planets Space* **58,** 1587–1592.

Usami, T. (2003). *Materials for Comprehensive List of Destructive Earthquakes in Japan, [416]-2001*, Univ Tokyo Press, Tokyo (in Japanese).

Usami, T., and Daiwa Exploration and Consulting Co. Ltd. (Editor). (1994). *Seismic Intensity Distributions of Historical Earthquakes in Japan*, Japan Electric Association, Tokyo (in Japanese).

Wessel, P., and W. H. F. Smith (1998). New, improved version of generic mapping tools released, *Eos Trans. Am. Geophys. Union* **79,** 579.

Earthquake Research Institute
University of Tokyo
1-1-1 Yayoi, Bunkyo-ku
Tokyo 113-0032, Japan
mmiyazaw@eri.u-tokyo.ac.jp
(M.M.)

Disaster Prevention Research Institute
Kyoto University
Gokasho, Uji
Kyoto 611-0011, Japan
mori@eqh.dpri.kyoto-u.ac.jp
(J.M.)

Manuscript received 4 September 2008